Biosensors and Bioelectronics 41 (2013) 110–115

Contents lists available at SciVerse ScienceDirect

Biosensors and Bioelectronics

journal homepage: www.elsevier.com/locate/bios

NiO nanoparticle-based urea biosensor

Manisha Tyagi [a], Monika Tomar [b], Vinay Gupta [a,*]

[a] Department of Physics and Astrophysics, University of Delhi, Delhi 110007, India
[b] Physics Department, Miranda House, University of Delhi, Delhi 110007, India

ARTICLE INFO

Article history:
Received 29 April 2012
Received in revised form
18 July 2012
Accepted 27 July 2012
Available online 17 August 2012

Keywords:
NiO nanoparticles
Electrocatalytic
Urea
Biosensor

ABSTRACT

NiO nanoparticles (NiO-NPs) have been exploited successfully for the fabrication of a urea biosensor. A thin film of NiO nanoparticles deposited on an indium tin oxide (ITO) coated glass substrate serves as an efficient matrix for the immobilisation of urease (Ur), the specific enzyme for urea detection. The prepared bioelectrode (Ur/NiO-NP/ITO/glass) is utilised for urea sensing using cyclic voltammetry and UV–visible spectroscopy. NiO nanoparticles act as electro-catalytic species that are based on the shuttling of electrons between Ni^{2+} and Ni^{3+} in the octahedral site and result in an enhanced electrochemical current response. The prepared bioelectrode (Ur/NiO-NPs/ITO/glass) exhibits a high sensitivity of 21.3 μA/(mM * cm^2) and a good linearity in a wide range (0.83–16.65 Mm) of urea concentrations with fast response time of 5 s. The low value of the Michaelis-Menten constant (K_m=0.34 mM) indicates the high affinity of Ur towards the analyte (urea). The high catalytic activity, along with the redox behaviour of NiO-NPs, makes it an efficient matrix for the realisation of a urea biosensor.

1. Introduction

Urea, an end product of nitrogen metabolism, has a great significance in clinical processes, in addition to being a crucial indicator of liver and kidney function. High urea concentrations (normal level in the serum is 1.33–3.33 mM) cause renal failure (acute or chronic), urinary tract obstruction, dehydration, shock, burns and gastrointestinal bleeding (Rajesh et al., 2005; Dhawan et al., 2009). Low urea concentrations are related to hepatic failure, nephritic syndrome, cachexia (low-protein and high-carbohydrate diets), etc. (Rajesh et al., 2005; Dhawan et al., 2009). Hence, it is of utmost interest to develop cost-effective techniques for real-time monitoring of urea in human serum, including urine and blood samples. A number of transducers have been used for detection of urea including amperometric, potentiometric, optical, thermal, and piezoelectric (Rajesh et al., 2005; Ahuja et al., 2011; Konck et al., 2001; Yang et al., 2007). Amongst them, the urease-based amperometric biosensor is the most promising approach, because it offers a fast, simple, and low-cost detection technique. The response time of such a biosensor is directly associated with the hydrolysis rate of urea on the electrode surface; therefore, rapid production of NH^{4+} ions on the electrode will lead to a highly sensitive biosensor. Several matrices such as conducting polymers, metal nanoparticles, metal oxides, etc., have been used to immobilise urease for the fabrication of urea biosensors (Dhawan et al., 2009; Krajewska (2009); Wang et al., 2007). Recently, metal oxide nanoparticles and nanostructures have aroused the interest of the research community as an efficient matrix for biosensors due to the flexibility in obtaining the desired properties, such as an optimum surface-to- volume ratio, a high catalytic efficiency, and an ability to absorb biomolecules (Feng et al., 2006; Das et al., 2010). Amongst them, nickel oxide (NiO), due to its high electrocatalytic properties, oxygen ion conductivity, biocompatibility, nontoxicity, high chemical stability, and high electron transfer feature, is a promising candidate for the development of biosensors (Li et al., 2008; Salimi et al., 2007). The high isoelectric point (IEP=10.7) of NiO is also advantageous in binding biomolecules that have a low IEP via strong electrostatic interaction. NiO thin films and their composites have been efficiently used for the development of various biosensors for the estimation of haemoglobin, glucose, metformin, uric acid and sulphide in desired test specimens (Salimi et al., 2007; Zang et al., 2010; Safavi et al., 2009; Sattarahmady et al., 2010). However, no attempt has been made to fabricate urea biosensors that are based on NiO. Moreover, there is no report on the fabrication of an amperometric urea biosensor based on a metal oxide nanoparticle electrode without an external mediator. Pratima et al. have studied the zinc oxide-chitosan nanobiocomposite-based matrix for the detection of urea using $FeCN_6^{3-/4-}$ as an external mediator (Solanki et al., 2008). NiO has its own redox couple, which may be exploited for the

* Corresponding author. Tel.: +919811563101.
E-mail addresses: drguptavinay@gmail.com, drvin_gupta@rediffmail.com (V. Gupta).

0956-5663/$ - see front matter © 2012 Elsevier B.V. All rights reserved.
http://dx.doi.org/10.1016/j.bios.2012.07.062

fabrication of an efficient urea biosensor without using any external mediator. Because NH^{4+} ions are not electroactive, they are oxidised to nitrogen molecules via two approaches: either using a second enzyme or a catalytically active species (Solanki et al., 2008; Rodriguez et al., 2004). A few reports have demonstrated an amperometric urea biosensor using two enzymes: urease and isocitrate dehydrogenase (Rodriguez et al., 2004) or glutamate dehydrogenase. Kaushik et al. have demonstrated an iron oxide-chitosan nanobiocomposite-based matrix for an amperometric urea biosensor using two enzymes, namely, urease and glutamate dehydrogenase (Kaushik et al., 2009). The dual-enzyme- based biosensor suffers from disadvantages, such as a complex structure and higher sensor cost. Alternatively, Mishima et al. developed an amperometric urea biosensor that was based on a platinum–iridium electrode using a single enzyme and the electrocatalytic properties of iridium (Mishima et al., 1998). However, the main disadvantages of these electrodes are the saturation and fast poisoning of the metal catalytic surface, due to ammonia ions, after repeated measurements. The high catalytic efficiency of NiO nanoparticles precludes the need for a second enzyme. Furthermore, NiO nanoparticles solve the poisoning problem that has been observed on the metal electrodes. As a result, the NiO-based bioelectrode may be advantageous for the fabrication of a low cost urea biosensor. In the present work, NiO nanoparticles have been exploited for the fabrication of an attractive biocompatible matrix for a urea biosensor. Urease has been successfully immobilised on the surface of the NiO matrix by a physical adsorption technique for specific detection of urea.

2. Experimental

2.1. Materials

Urease (Ur) (from jack beans), potassium iodide and mercury (II) chloride were purchased from Sigma-Aldrich. Sodium phosphate monobasic anhydrous and sodium phosphate dibasic dihydrate were obtained from Sisco Chemical, India. All chemicals were used without further purification. Deionised water (resistivity = 18.2 MΩ cm^{-1}) was used for the preparation of aqueous solutions.

2.2. Preparation of solutions

Ur (1 mg/ml) was freshly prepared in PBS buffer (pH = 7.0). Different concentrations of urea solution (0.83–16.65 mM) were freshly prepared in deionised water.

2.3. Preparation of NiO thin film and immobilisation of Ur

NiO nanoparticles were synthesised using a two step procedure. First, 4.35 g of $Ni(OAc)_2 \cdot 4H_2O$ and 1.5 g of NaOH were dissolved in 30 ml and 75 ml of distilled water, respectively, in separate containers, followed by coprecipitation using polyvinylpyrrolidone (0.5 g) as a surfactant (Singh et al., 2011). The precipitate was collected by centrifugation, thoroughly washed with deionised water and ethanol several times, and then dried at 50 °C for 24 h. In the second step, the collected precipitate was calcined at 300 °C for 2 h, resulting in the removal of organic compounds and the formation of NiO nanoparticles. The NiO nanoparticles were ultrasonically dispersed in 5 ml methanol at room temperature. Thin films of NiO nanoparticles (Nano-NiO) were fabricated by uniformly spreading a 20 µl solution of NiO nanoparticles dispersed in methanol onto the surface of an ITO coated Corning glass (ITO/glass) substrate. ITO/glass substrates of 2 cm × 1 cm area were used; for electrical contact of the electrode, a 1 cm × 1 cm area was masked prior to the film deposition.

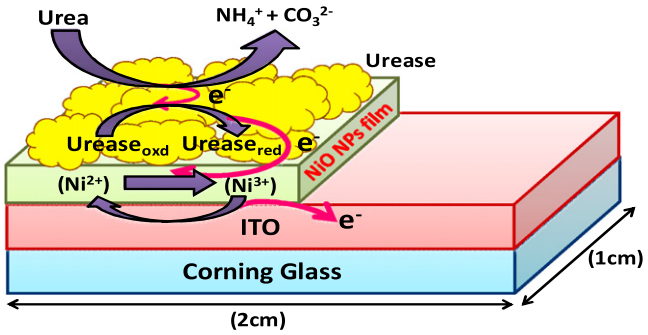

Fig. 1. Schematic of the prepared Ur/NiO-NP/ITO/glass bioelectrode.

This process was repeated five times; the resulting electrode was dried overnight at room temperature, followed by washing with deionised water to remove any unbound particles. A low IEP (~5.0) solution of 10 µl of urease (1.0 mg/ml, in phosphate buffer, 50 mM, pH 7.0) was successfully immobilised on the surface of the NiO thin film (IEP = 10.7) via a physical adsorption technique: the prepared bioelectrode (Ur/NiO-NP/ITO/glass) was kept overnight for drying. A schematic of the prepared bioelectrode with the sensing mechanism is shown in Fig. 1.

2.4. Measurement and apparatus

The size, shape and crystallinity of the synthesised NiO nanoparticles (NPs) were studied using a transmission electron microscope (TEM) (FEI TECNAI $G^2$30-U-TWIN). X-ray diffraction (XRD) (Bruker D8 Discover) studies were conducted to identify the crystallographic structure of the prepared NiO nanoparticle thin films. Atomic force microscopy (AFM) (Veeco DICP2) was used to study the surface morphology of the prepared samples. A Fourier transform infrared (FTIR) (Perkin Elmer) spectrophotometer was used to characterise the NiO-NPs thin film and its interaction with urease. For the FTIR studies, NiO-NPs thin films were prepared on the KBr pellets. Electrochemical analysis was conducted on a Gamry Reference 600 Potentiostat/Galvanostat using a conventional three-electrode cell configuration in a phosphate buffered saline (PBS) solution (50 mM, pH 7.0, 0.9% NaCl) with Ag/AgCl as the reference electrode and Pt foil as the counter electrode. The apparent enzyme activity of the bioelectrode was also studied using a UV–visible spectrophotometer (Perkin Elmer, Lambda 35).

3. Results and discussion

3.1. Morphological and structural studies

Fig. 2(a) shows the TEM image of the calcined NiO nanoparticles at low magnification. The synthesised NiO nanoparticles are well monodispersed, having an average diameter of approximately 12 nm. The indexed selected area electron diffraction (SAED) pattern of the NiO-NPs is shown in Fig. 2(b), indicating that the NPs are polycrystalline having (220), (200) and (111) planes. The observed SAED pattern was indexed on the basis of the Fm3m space group. The HRTEM image of a NiO nanoparticle, shown in Fig. 2(c), shows a lattice spacing of 2.10 Å, which corresponds to the interplanar distance between the (200) planes. The estimated value of the lattice constant 'a' is approximately 4.20 Å.

Fig. 3 shows the X-ray diffraction pattern of the NiO-NPs thin film. The NPs thin film is polycrystalline, having XRD peaks corresponding to (111), (200) and (220) reflections of the cubic (fcc) phase of NiO with lattice parameter $a = 4.21$ Å

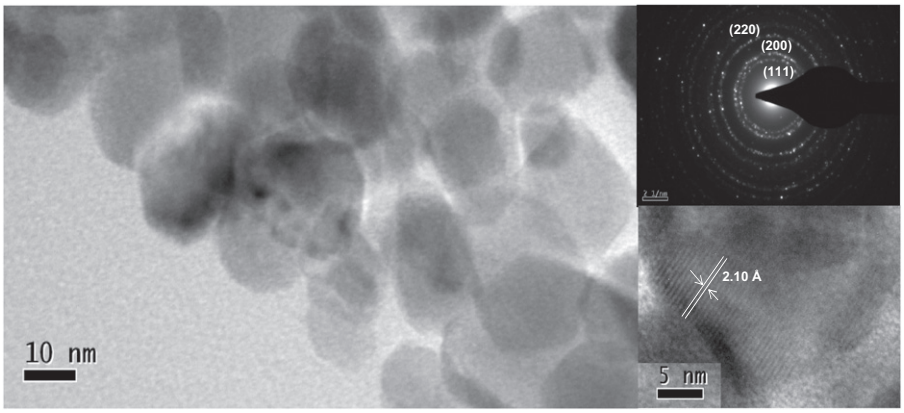

Fig. 2. (a) TEM image of the NiO nanoparticles. (b) Electron diffraction pattern of the NiO nanoparticles. (c) HRTEM image of the nanoparticles at 5 nm resolution.

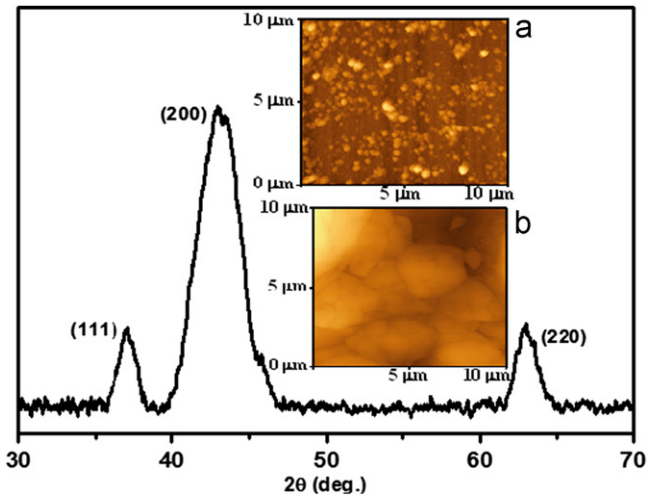

Fig. 3. X-ray diffraction pattern of the NiO-NP thin film. The inset shows an AFM image of the (a) NiO-NP/ITO/glass electrode and (b) Ur/NiO-NP/ITO/glass bioelectrode.

(space group: *Fm*3*m*). The value of 'a' is slightly higher than the corresponding bulk value (4.177 Å) and is associated with the presence of tensile stress in the NPs film (JCPDS 47–1049). The observed XRD results on crystallinity and lattice constant are in agreement with the SAED data (Fig. 2) obtained for the NiO nanoparticles. The observed broadening in the XRD peaks (Fig. 3) indicates the nanosize nature of the NiO grains. The crystallite size of the NiO-NPs thin film is calculated from the dominant (200) XRD peak using the Debye–Scherrer formula. The value of crystallite size (~4 nm) is much lower than the corresponding value determined from the TEM analysis, indicating that the NiO-NPs are comprised of a number of crystallites.

The inset of Fig. 3(a and b) shows the AFM images of the surface of the NiO-NP thin film and the urease (Ur) immobilised (Ur/NiO-NP/ITO/glass) bioelectrode, respectively. A granular, porous morphology for the surface of the NiO-NPs thin film was observed (inset of Fig. 3(a)). The homogeneous globular morphology increases due to the immobilisation of a macromolecular enzyme (Ur) on the NiO-NP surface, as shown in the inset of Fig. 3(b). The surface roughness of the NiO-NP thin film also increases from 10 nm to 30 nm after the immobilisation of Ur. The increased grain size and surface roughness obtained for Ur/NiO-NPs/ITO/Glass bioelectrode confirm the successful immobilisation of urease on the surface of NiO-NPs thin film matrix.

3.2. FTIR spectroscopy

Supplementary Fig. 1(a) shows the FTIR spectra of the NiO-NP thin film deposited on a KBr pellet. The absorption bands observed at 664 and 463 cm^{-1} (Suppl. Fig. 1(a)) are assigned to the stretching vibration and the torsional vibration modes of the Ni–O bond at the tetrahedral and the octahedral sites, respectively (Arora et al., 2011). The band at 556 cm^{-1} corresponds to the stretching mode of the Ni–O–Ni bond (Arora et al., 2011). The wide absorption band observed at 3450 cm^{-1} corresponds to the stretching vibration mode of the O–H group, and the mode at 1632 cm^{-1} is the O–H bending band, which is associated with the adsorbed water molecules on the surface of thin film sample. The band observed at 1041 cm^{-1} is also attributed to the stretching vibration mode of the hydroxyl group (Arora et al., 2011). The FTIR spectra of the Ur/NiO-NP/KBr sample (curve (b) of Suppl. Fig. 1) shows that the absorption band due to stretching mode of the Ni–O–Ni bond is shifted to a slightly higher frequency (~572 cm^{-1}) after the immobilisation of urease and may be associated with the electrostatic interaction between the NiO and urease. The bands observed at 1659 cm^{-1} and 1567 cm^{-1} are attributed to the N–H deformation mode in amide II and the N–H bending modes of amide I bands respectively, while the band observed at 1080 cm^{-1} is due to the stretching vibration mode of the hydroxyl group (Kaushik et al., 2009). The results confirm the successful immobilisation of urease on the surface of NiO-NP thin film.

3.3. Photometric enzyme assay

The apparent enzyme activity of the Ur/NiO-NPs/ITO/glass bioelectrode has been determined using a photometric enzyme assay. Ur catalyses the hydrolysis of urea to produce ammonia, which in turn reacts with Nessler's reagent to form a coloured product, $NH_2Hg_2I_3$ (Tiwari et al., 2009). The prepared bioelectrode was dipped for 2 min in 3.17 ml of PBS solution (pH 7.0), containing 10 µl of Nessler's solution and 100 µl of analyte (urea) in varying concentration (0.83 to 16.65 mM). The difference between the initial and final absorbance of the bioelectrode at a fixed wavelength of 385 nm, was measured, and the corresponding values are plotted in Fig. 4 as a function of urea concentration. The enzyme activity of the bioelectrode increases linearly with increasing urea concentrations up to 8.32 mM (Fig. 4) and thereafter showed saturation. The apparent enzyme activity, i.e., the amount of enzyme bound on the surface of the NiO-NP thin film matrix, has been calculated using the equation $a_{app}^{enz}(Ucm^{-2}) = AV/\varepsilon ts$, where A is the difference in absorbance before and after incubation of the saturated solution, V is the total volume

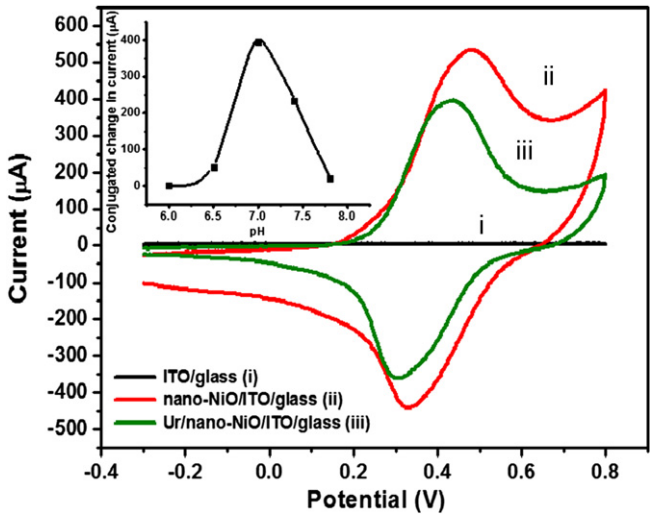

Fig. 4. Photometric study of the prepared Ur/NiO-NPs/ITO/glass bioelectrode. The inset shows the interference study of the Ur/NiO-NPs/ITO/glass bioelectrode.

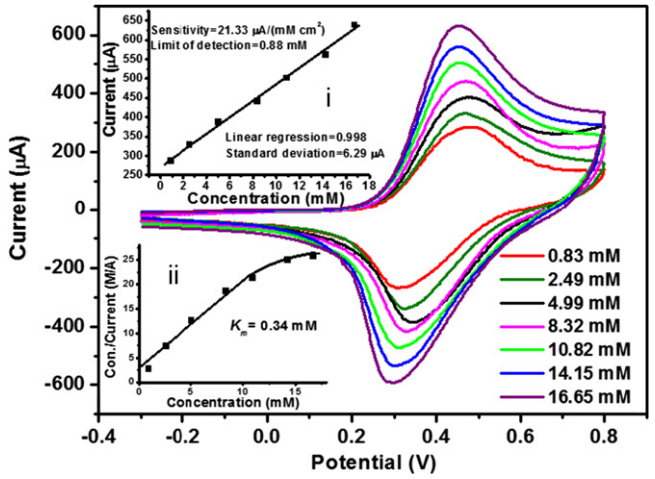

Fig. 5. Cyclic voltammogram of the ITO/glass substrate (curve i), NiO-NP/ITO/glass electrode (curve ii) and Ur/NiO-NP/ITO/glass bioelectrode (curve iii) in a PBS buffer without an external mediator. The inset shows the effect of the pH of PBS on the peak oxidation current of the Ur/NiO-NP/ITO/glass bioelectrode.

(3.17 cm^3), ε is the millimolar extinction coefficient of Nessler's reagent, t is the reaction time (2 min) and s is the surface area of the electrode (Tiwari et al., 2009). The estimated value of the apparent enzyme activity was approximately 4.3×10^{-1} Ucm^{-2}, indicating the higher activity of the immobilised Ur on the surface of NiO nanoparticle matrix. The value of the apparent enzyme activity obtained in the present case is higher than that reported for NiO based matrices used for detecting other biomolecules, such as uric acid (Arora et al., 2011).

3.4. Electrochemical studies

Fig. 5 shows the cyclic voltammetric (CV) spectra of the (i) ITO/glass substrate (ii) NiO-NPs/ITO/glass electrode and (iii) Ur/NiO-NPs/ITO/glass bioelectrode. Fig. 5 shows that in PBS solution (without an external mediator), the ITO/glass substrate does not show any oxidation or reduction peaks over the measured potential window (−0.3 V to 0.8 V) due to the absence of any redox couple in the electrolyte or in the electrode. With the NiO-NP thin film, deposited on the surface of the ITO/glass substrate (NiO-NP/ITO electrode), well defined oxidation and reduction peaks are observed in the CV spectra (curve (ii) in Fig. 5) using a PBS solution without an external mediator. The presence of redox peaks without using an external mediator is because NiO possesses a redox couple ($Ni^{2+}\leftrightarrow Ni^{3+}$). Water molecules present in PBS solution are strongly adsorbed on the surface of NiO-NPs where oxygen act as a proton-acceptor site for the water molecule through hydrogen bonding, leading to conversion of surface NiO to the hydroxide phase $Ni(OH)_2$ (Medway et al., 2006; Nakamura et al., 2005) as:

$$NiO+H_2O\ (\text{physisorbed})\rightarrow NiOH_2O\rightarrow Ni(OH)_2$$

However, the amount of $Ni(OH)_2$ spontaneously formed at the surface due to the interaction of H_2O is limited and scanning the electrode up to a high potential at 0.8 V leads to the conversion of more NiO to $Ni(OH)_2$, and then to NiOOH. The anodic peak is then due to the oxidation of the $Ni(OH)_2$ phase to NiO(OH) whilst the corresponding cathodic peak represents the reduction of NiO(OH) to $Ni(OH)_2$ and hence a pair of redox peak appears (Fig. 5). The peak oxidation current of approximately 540 μA was obtained at a relatively lower potential (~0.47 V). The separation between the peak oxidation and reduction currents (curve (ii) in Fig. 5) is very small (0.13 V) and is attributed to the fast electron communication characteristics of the fabricated matrix (NiO-NPs thin film). The peak oxidation current decreased significantly (~400 μA) upon immobilisation of Ur onto the surface of the NiO-NPs/ITO/glass electrode (curve (ii) in Fig. 5). The decrease in oxidation current is attributed to the non-conducting nature of the macromolecular enzyme (urease). The inset in Fig. 5 shows the variation in the peak oxidation current of the Ur/NiO-NPs/ITO/glass bioelectrode as a function of the pH of the buffer solution. The bioelectrode shows the maximum peak oxidation current and a maximum activity at a pH of 7.0.

To determine the surface concentration of the ionic species on the Ur/NiO-NP/ITO/glass bioelectrode, CV studies have been conducted as a function of scan rate (ν) from 10 to 100 mV/s (supplementary Fig. 2). Both the anodic (I_{pa}) and cathodic (I_{pc}) peak currents increase linearly with the scan rate (ν) as shown in the inset of supplementary Fig. 2. The linear increase in redox current with ν suggests that the reaction occurring at the surface of the bioelectrode is a surface controlled electrode process (Salimi et al., 2007). The peak height also varies directly with the sweep rate (inset of supplementary Fig. 2), indicating improved electrocatalytic behaviour. The surface concentration of the ionic species (I^*) on the Ur/NiO-NPs/ITO/glass bioelectrode is estimated using the Brown–Anson model based on the following equation (Arora et al., 2011):

$$I_{pa}=\frac{n^2F^2I^*Av}{4RT} \quad (1)$$

where n is the number of electrons transferred (1), F is the Faraday constant (96485 C/mol), R is the gas constant (8.314 J mol^{-1} K^{-1}), A is the surface area of the bioelectrode (1 cm^2), ν is scan rate, and T is the temperature (300 K). The estimated value of the surface concentration of the ionic species (I^*) on the Ur/NiO-NPs/ITO/glass bioelectrode is approximately 1.4×10^{-8} mol cm^{-2} which is higher than the corresponding value reported for the urea biosensor using another matrix (Solanki et al., 2008). The higher value of surface concentration reveals that large numbers of redox species are available in the prepared bioelectrode for oxidation, leading to higher Faradic current. This result may be attributed to the presence of NiO nanoparticles that result in an increased electron transfer process.

The value of the electron transfer rate constant (k_s) for urease immobilised on the NiO-NP/ITO/glass electrode can also be

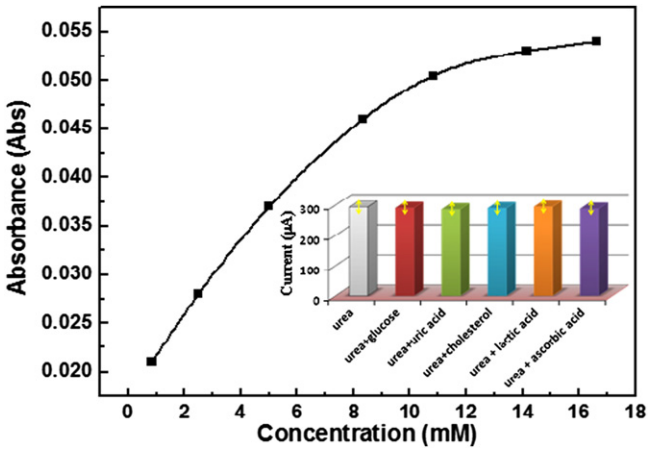

Fig. 6. Sensing response of the Ur/NiO-NP/ITO/glass bioelectrode as a function of urea concentration (0.83–16.65 mM);. Inset: (i) variation of the peak oxidation current as a function of urea concentration and (ii) Hanes plot between the analyte concentration and analyte concentration/current.

calculated using the Laviron model given by the following equation (Laviron (1979)):

$$k_s = \frac{\Delta E_p n F \nu}{RT} \quad (2)$$

where ΔE_p is the peak separation potential. The estimated value of k_s obtained using eq. (2) is approximately 5.3 s^{-1} (T=300 K, n =1, ΔE_p=0.13 V and ν=70 mV) and is higher than the corresponding value reported for other nanoparticle based bioelectrodes. The results indicate that the fast transfer of electrons is generated during a biochemical reaction from the immobilised Ur to the ITO electrode through the NiO nanoparticles (Kaushik et al., 2009; Zhang et al., 2005).

The sensing response characteristics of the prepared Ur/NiO-NPs/ITO/glass bioelectrode were obtained as a function of the urea concentrations from 0.83 to 16.65 mM (1.33–3.33 mM is the physiological range), and are shown in Fig. 6. The schematic of the biochemical reaction occurring at Ur/NiO-NPs/ITO/glass bioelectrode is shown in Fig. 1. Urease oxidises the urea in the solution and in the process it gets reduced. The reduced urease donates the excess electron to the NiO-NPs matrix to reduce the redox species. The NiO-NPs matrix reoxidizes by transferring the electron to the external circuit due to efficient electron transfer and good redox property of prepared nanoparticles bio-matrix and resulting in enhancement of the current (Fig. 1). Whereas, during the reverse scan of the voltamogram the process repeat in an opposite manner. Hence, catalytic oxidation of urea by urease involves gain or loss of electrons from a molecule thus completing a redox reaction. Fig. 6 shows that the peak oxidation current increases with successive addition of urea in the buffer solution. The increase in current with increasing concentration of urea is attributed to the increase in the number of released electrons during oxidation of urea. This result may be attributed to the NiO nanoparticles in the bioelectrode acting as good acceptors of the electrons generated during reoxidation of Ur, which are transferred underneath the ITO electrode via the Ni^{+2}/Ni^{+3} redox couple, resulting in an increased electrochemical current response. The magnitude of the oxidation peak current increased linearly from 289 μA to 640 μA with an increase in the urea concentration from 0.83 mM to 16.65 mM (inset in Fig. 6). In order to confirm that the urease is responsible of the catalytic current in the presence of substrate, a control experiment was carried out in which sensing response for urea was also studied without immobilisation of urease on the surface of NiO-NPs/ITO/glass electrode. It is important to point out that no increase in oxidation and reduction currents were observed in the CV with increase in urea concentration from 0.83 to 16.65 mM indicating that the oxidation of urea does not occur at the surface of the transducer (NiO-NPs/ITO/glass). Thus, increase in CV current observed in the biosensing reaction involving Ur/NiO-NPs/ITO/glass bio-electrode with varying urea concentrations is solely due to the bio-electrocatalytic oxidation of urea in the presence of immobilised urease and not due to the direct oxidation of urea in the presence of substrate. Urease oxidises the urea in the solution and in the process it gets reduced. The reduced urease donates the excess electron to the NiO-NPs matrix to reduce the redox species. The NiO-NPs matrix reoxidizes by transferring the electron to the external circuit due to efficient electron transfer and good redox property of the prepared nanoparticles bio-matrix thus resulting in enhancement of the current (Fig. 1). Whereas, during the reverse scan of the voltamogram the process repeat in an opposite manner. Hence, catalytic oxidation of urea by urease involves gain or loss of electrons from a molecule thus completing a redox reaction. The increase in current with increasing concentration of urea is attributed to the increase in the number of released electrons during oxidation of urea. The NiO-NPs have been synthesised in different batches under similar processing conditions and have been utilised for preparation of bioelectrodes. The proposed bioelectrode exhibits same response characteristics for fixed concentration of urea within an accuracy of ± 5% confirming the good reproducibility of sensor properties.

The sensitivity of the Ur/NiO-NPs/ITO/glass bioelectrode is approximately 21.33 μA/(mM cm^2) with a linear regression coefficient of 0.998 and a standard deviation of 6.29 μA. The sensitivity is much higher than the corresponding value reported for other metal oxide nanoparticles and polymer membrane based amperometric urea biosensors (Solanki et al., 2008; Kaushik et al., 2009; Velichkova et al., 2011) (Suppl. Table 1). The high sensitivity of the Ur/NiO-NPs/ITO/glass bioelectrode in the present work is attributed to the high electrocatalytic activity of the NiO nanoparticles. The prepared Ur/NiO-NPs/ITO/glass bioelectrode exhibits a fast response time of 5 s with high reproducibility. The value of the Michaelis-Menten kinetic parameter (K_m) for the Ur/NiO-NPs/ITO/glass bioelectrode, is estimated from the Hanes plot shown in inset (ii) of Fig. 6 (Saha et al., 2009). The estimated value of K_m is approximately 0.34 mM, which is much lower than the reported values for urea biosensors developed by other workers (Solanki et al., 2008; Kaushik et al., 2009; Velichkova et al., 2011) (Suppl. Table 1). The low K_m value of the prepared bioelectrode indicates that the immobilised urease has a higher affinity towards its analyte (urea). This finding may be attributed to the higher loading of urease on the surface of the NiO-NP thin film in a favourable orientation.

3.5. Interference and shelf life analysis

The selectivity of the Ur/NiO-NPs/ITO/glass bioelectrode towards urea (Inset of Fig. 4) has also been studied. The CV response was taken after adding a normal concentration of urea (1 mM) with different interferants: glucose (5.6 mM), uric acid (0.1 mM), cholesterol (5 mM), lactic acid (5 mM) and ascorbic acid (0.05 mM). The concentrations of glucose, uric acid, cholesterol, lactic acid and ascorbic acid are based on their normal physiological values in human serum. The results indicate that the bioelectrode (Ur/NiO-NPs/ITO/glass) in the present work has a maximum interference of approximately 2.7% in the presence of uric acid and that the effect of other interferents is less than 2.0%.

The shelf-life of the Ur/NiO-NPs/ITO/glass bioelectrode was determined by measuring its response at a regular interval of time (upto 20 weeks) as shown in supplementary Fig. 3. The prepared

bioelectrode retains an approximately 84% response even after 20 weeks when stored at 4 °C, which is much higher than earlier reported results on bioelectrodes that are based on other metal oxide nanostructures (Kaushik et al., 2009; Velichkova et al., 2011) (Suppl. Table 1).

4. Conclusion

In summary, a NiO nanoparticle based bioelectrode has been exploited successfully for the realisation of an efficient urea biosensor. The prepared bioelectrode (Ur/NiO-NPs/ITO/glass) exhibits improved linearity over a wide detection range (0.83–16.65 mM), a high sensitivity of 21.33 μA/(mM cm^2), a high apparent enzyme activity of 4.3×10^{-1} U/cm^2, a fast response time of 5 s and a long shelf life of 20 weeks. The low K_m value of 0.34 mM indicates a high affinity of the immobilised urease on the surface NiO-NPs/ITO electrode for urea. The NiO nanoparticle based matrix used in the present work ensures a suitable active surface with its own redox couple ($Ni^2 \leftrightarrow Ni^{3+}$) for enhanced urease immobilisation, favourable conformation, and fast electron transfer which catalyses the electrochemical oxidation of ammonia.

Acknowledgements

The authors are thankful to the UGC, DRDO, DST and the government of India for the financial support to conduct this research work. One of the authors (MT) is acknowledges CSIR and the University of Delhi for a research fellowship.

Appendix A. Supporting information

Supplementary data associated with this article can be found in the online version at http://dx.doi.org/10.1016/j.bios.2012.07.062.

References

Ahuja, T., Kumar, D., Singh, N., Biradar, A.M., Rajesh, 2011. Materials Science and Engineering C 31, 90.
Arora, K., Tomar, M., Gupta, V., 2011. Biosensors and Bioelectronics 30, 333.
Das, M., Sumana, G., Nagarajan, R., Malhotra, B.D., 2010. Applied Physics Letters 96, 133703.
Dhawan, G., Sumana, G., Malhotra, B.D., 2009. Journal of Biochemical Engineering 44, 42.
Feng, K.J., Yang, Y.H., Wang, Z.J., Jiang, J.H., Shen, G.L., Yu, R.Q., 2006. Talanta 70, 561.
Kaushik, A., Solanki, P.R., Ansari, A.A., Sumana, G., Ahmad, S., Malhotra, B.D., 2009. Sensors and Actuators B 138, 572.
Konck, R., Lenarczuk, T., Radomska, A., Glab, S., 2001. Analyst 126, 1080.
Krajewska, B., 2009. Journal of Molecular Catalysis B: Enzymatic 59, 9.
Laviron, E.J., 1979. Journal of Electroanalytical Chemistry 101, 19.
Li, C., Liu, Y., Li, L., Du, Z., Xu, S., Zhang, M., Yin, X., Wang, T., 2008. Talanta 77, 455.
Medway, S.L., Lucas, C.A., Kowal, A., Nichols, R.J., Johnson, D., 2006. Journal of Electroanalytical Chemistry 587, 172.
Mishima, B.A., Lescano, D., Holgado, M.T., Mishima, H.T., 1998. Electrochimica Acta 41, 395.
Nakamura, M., Tanaka, M., Ito, M., Sakata, O., 2005. Journal of Chemical Physics 122, 224703.
Rajesh, Bisht, V., Takashima, W., Kaneto, K., 2005. Biomaterials 26, 3683.
Rodriguez, B.B., Bolbot, J.A., Tothill, I.E., 2004. Analytical Letters 37 (3), 415.
Safavi, A., Maleki, N., Farjami, E., 2009. Biosensors and Bioelectronics 24, 1655.
Saha, S., Arya, S.K., Singh, S.P., Sreenivas, K., Malhotra, B.D., Gupta, V., 2009. Biosensors and Bioelectron 24, 2040.
Salimi, A., Sharifi, E., Noorbakhsh, A., Soltanian, S., 2007. Biophysical Chemistry 125, 540.
Sattarahmady, N., Heli, H., Faramarzi, F., 2010. Talanta 82, 1126.
Singh, J., Kalita, P., Singh, M.K., Malhotra, B.D., 2011. Applied Physics Letters 98, 123702.
Solanki, P.R., Kaushik, A., Ansari, A.A., Sumana, G., Malhotra, B.D., 2008. Applied Physics Letters 93, 163903.
Tiwari, A., Aryal, S., Pilla, S., Gong, S., 2009. Talanta 78, 1401.
Velichkova, Y., Ivanov, Y., Marinov, I., Ramesh, R., Kamini, N.R., Dimcheva, N., Horozova, E., Godjevargova, T., 2011. Journal of Molecular Catalysis B: Enzymatic 69, 168.
Wang, X., Watanabe, H., Sekioka, N., Hamana, H., Uchiyama, S., 2007. Electroanalysis 19, 1300.
Yang, Z., Si, S., Dai, H., Zhang, C., 2007. Biosensors and Bioelectronics 22, 3283.
Zang, De W., Jin, C., Chuan, J.L., Xiang, Y.Y., Qi, Z.J., 2010. Mikrochimica Acta 168, 259.
Zhang, L., Jiang, X., Wang, E., Dong, S., 2005. Biosensors and Bioelectronics 21, 337.